

Report LR-803

Inverse 3-D Aerodynamic Design over the Flight Envelope

April 1996

J. Middel


TU Delft

Delft University of Technology

Faculty of Aerospace Engineering

Inverse 3-D Aerodynamic Design over the Flight Envelope

J. Middel

Copyright © 1996, by Delft University of Technology, Faculty of Aerospace Engineering, Delft, The Netherlands.

All rights reserved. No part of this publication may be reproduced, stored in a retrieval system or transmitted in any form or by any means, electronic, mechanical, photocopying, recording or otherwise, without the prior written permission of the Delft University of Technology, Faculty of Aerospace Engineering, Delft, The Netherlands.


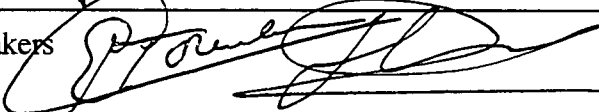
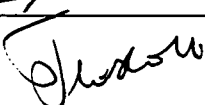
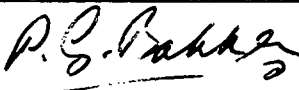
Publisher: Delft University of Technology
Faculty of Aerospace Engineering
P.O. Box 5058
2600 GB Delft
The Netherlands.
tel: (015)782058
fax: (015)781822

Date April 96

Report LR - 803

ISBN: 90-5623-037-0

Title	:	Inverse 3-D Aerodynamic Design over the Flight Envelope.
Author(s)	:	J. Middel
Abstract	:	A tool for the aerodynamic design of complex three dimensional configurations with prescribed surface pressure distributions is presented. It is basically a procedure to determine amplitudes of (local) changes of a baseline geometry that yields a best fit through user prescribed target pressure distributions, considering a series of flight conditions. This method is based on a 3-D linear potential flow (panel) method and grants the user full control over where and how the geometry is changed. An example case is provided.
Keyword(s)	:	aircraft aerodynamic design, inverse aerodynamics, potential flow, panel method.

Date	May 1996
Prepared	J. Middel 
Verified	H.W.M. Hoeijmakers E. Torenbeek 
Approved	Th. van Holten 
Authorized EB	P.G. Bakker  27-06-96

1 - Summary.

A tool for the aerodynamic design of complex three dimensional configurations with prescribed surface pressure distributions is presented. It is basically a procedure to determine amplitudes of (local) changes of a baseline geometry that yields a best fit through user prescribed target pressure distributions, considering a series of flight conditions. This method is based on a 3-D linear potential flow (panel) method and grants the user full control over where and how the geometry is changed. An example case is provided.

2 - Nomenclature.

A	-	area
A_{ishape}	-	amplitude of basic shape function
F	-	object function
M_{∞}	-	free stream Mach number
U_{∞}	-	free stream velocity
W	-	weight factor
c_p	-	pressure coefficient
$g(s,t)$	-	geometry wetted surface
k	-	relaxation factor
m	-	mass flux
\hat{n}	-	normal vector
s, t	-	surface coordinates spanning wetted surface
u_n	-	normal velocity
w	-	normal velocity at lifting surface
x, y, z	-	coordinates
z_c	-	camber
z_t	-	thickness
α	-	angle of attack
γ	-	ratio of specific heats
ϕ	-	perturbation potential
θ	-	dihedral
'	-	local reference system

3 - Introduction.

One of the most important goals in aerodynamic design is to find an aircraft shape definition which fulfills requirements such as a high maximum lift coefficient and high critical Mach number, low cruise drag and an acceptable stability and stall progression. Whether these requirements are met largely depends on the pressure distributions in the conditions under consideration (design and off-design). Hence, the analysis and optimization of pressure distributions through local refinement of the aircraft geometry is an integral part of (aerodynamic) design. Many different methods have been proposed but most applications, contrary to the present method, are usually limited to a single design point⁽¹⁾.

4 - Problem definition.

In the inverse design case, one wants to find the geometry that generates a specified pressure distribution over the wetted surface. Because such geometry usually does not exist, one must be satisfied with the geometry that best approximates the target pressure distribution. Furthermore, the designer usually wants to have full control over (changes in) the geometry itself. Starting from a

baseline design, a new geometry (g), spanned by s and t , is defined with superimposed a set of basic shape functions (Δg) with as yet unknown amplitudes (A), in symbolic notation:

$$g_{\text{new}}(s, t) = g_{\text{baseline}}(s, t) + \sum_{\text{ishape} = 1}^{\text{all shapes}} A_{\text{ishape}} \Delta g_{\text{ishape}}(s, t) \quad (1)$$

Next, target pressures must be specified over user selected parts of the geometry. The number and location of these target pressures is, in principle, independent of the number and kind of basic shapes functions, as well as the geometrical location that is modified. Of course, it is dissuaded to specify target pressures over those parts of the geometry, where the pressure distribution is hardly affected by the geometrical changes elsewhere. Target pressures may be defined for more than one flight condition and at multiple locations, independent of each other. Weight factors are assigned to each flight condition and each target pressure location to state the relative importance.

Now the object function can be mathematically defined as:

$$F = \sum_{\text{icase} = 1}^{\text{all cases}} W_{\text{icase}} \sum_{\text{ipanel} = 1}^{\text{all panels}} W_{\text{ipanel}} \left(c_{p|_{\text{ipanel, icase}}}^{\text{best fit}} - c_{p|_{\text{ipanel, icase}}}^{\text{target}} \right)^2 \quad (2)$$

Here, W denote weight factors that are set by the user to stress the relative importance of a design case or position. The inverse problem is now reduced to finding the amplitudes A_{ishape} that minimizes the differences in the best and the target pressure distribution. The object function F and the geometry amplitudes are coupled using:

$$c_{p|_{\text{ipanel, icase}}}^{\text{best fit}} = c_{p|_{\text{ipanel, icase}}}^{\text{baseline}} + \sum_{\text{ishape} = 1}^{\text{all shapes}} A_{\text{ishape}} \frac{\partial c_{p|_{\text{ipanel, icase}}}}{\partial A_{\text{ishape}}} \quad (3)$$

Although the pressure distribution depends non-linearly on the geometry, a linear relation between the change in pressure and geometrical changes is assumed. This assumption is reasonable for small changes, typically the geometry change $g(s, t)$ is a few percent of s and t . After finding an estimate for the amplitudes, the new, updated geometry should be analyzed again.

This formulation grants the designer full authority over the geometry changes: The user selects the basic shape functions $\Delta g(s, t)$ and the location of application. Moreover, for each panel, additional geometrical constraints may be defined:

$$g_{\text{min}} \leq \sum_{\text{ishape} = 1}^{\text{all shapes}} A_{\text{ishape}} \Delta g_{\text{ishape}}(s, t) \leq g_{\text{max}} \quad (4)$$

As previously stated, this geometry design process is non-linear by nature: The pressure coefficient is a non-linear function of the geometry as well as of the basic shape functions. This calls for an iterative process in which the baseline geometry, its pressure distribution, and the derivatives of the pressures with respect to the shape functions are updated during the iteration cycles in which the shape amplitudes are calculated. To partially account for the non-linear effects, these amplitudes may be relaxed and constrained:

$$A_{\text{min}} \leq (A_{\text{ishape, new}} = A_{\text{ishape, old}} + k_{\text{relax}} \Delta A_{\text{ishape, estimated}}) \leq A_{\text{max}} \quad (5)$$

The design problem is tackled using a 3-D panel method coupled with a numerical optimization technique, with special measures taken to keep computational costs low.

5 - Panel method basics.

Panel methods have become essential tools in the aerodynamic design at sub-and supersonic flight regimes, featuring:

- Accurate and detailed representation of the geometry.
- Versatility.
- Good evaluation of the velocity and pressure distributions, provided the flight conditions and geometry justify the use of potential flow theory.
- High computational efficiency and low costs.

A description of the basics of panel methods, in particular (the relevant details of) the NL-RAERO⁽²⁾⁽³⁾ panel method, follows.

5.1 - Governing equations.

Panel methods are based on the linearized potential flow theory, governed by the Prandtl-Glauert equation:

$$(1 - M_\infty^2) \frac{\partial^2 \phi}{\partial x^2} + \frac{\partial^2 \phi}{\partial y^2} + \frac{\partial^2 \phi}{\partial z^2} = 0 \quad (6)$$

The local velocity vector \hat{u} is expressed as:

$$\hat{u} = (u, v, w) = \nabla(U_\infty x + \phi(x, y, z)) \quad (7)$$

The perturbation velocity is assumed to be small compared to the free stream velocity. The pressure coefficient is defined as:

$$c_p = \frac{2}{\gamma M_\infty^2} \left(\left(1 - \frac{\gamma-1}{2} M_\infty^2 \left(\frac{(U_\infty + \frac{\partial \phi}{\partial x})^2 + (\frac{\partial \phi}{\partial y})^2 + (\frac{\partial \phi}{\partial z})^2}{U_\infty^2} - 1 \right) \right)^{\frac{\gamma}{\gamma-1}} - 1 \right) \quad (8)$$

This expression may be simplified using a first or second-order expansion approximation.

5.2 - Boundary conditions.

To solve the potential ϕ , boundary conditions are imposed. A Neuman zero-normal flow boundary condition is imposed on the wetted surface, with u_n the prescribed normal flow component:

$$\hat{n} \cdot \nabla(U_\infty x + \phi(x, y, z)) = u_n \quad (9)$$

This condition is imposed straightforwardly at the wetted surface of the fuselage and other "thick" bodies. For the lifting surfaces, some simplifications are made. The lifting surfaces are assumed to be thin and mildly cambered, and to be at small angle of attack. This allows to shift the boundary conditions to a reference surface and to combine the boundary conditions at the suction and pressure sides.

This reference surface is taken as the plane parallel to the x-axis of the geometry coordinate reference system and passing through the leading edge of the wing (segment). The wing reference surface ends at the projection of the trailing edge of the wing onto this plane. The wake of the wing is taken as the extension of the wing reference surface from its trailing edge to infinity downstream, i.e. again parallel to the x-axis of the geometry coordinate system. The boundary condition on the planar wing reference surface is:

$$w'(x', y', 0) = -U_\infty \sin \alpha \cos \theta + U_\infty \cos \alpha \frac{\partial z'_c}{\partial x'} - w'_q(x', y', 0) \quad (10)$$

where w'_q denotes the normal component of the Cauchy principal value part of the velocity induced by the source distribution of the strength

$$q(s, t) = U_\infty \cos \alpha \frac{\partial z'_t}{\partial x'} \quad (11)$$

on the reference surface of the lifting surfaces. The single quote denotes the reference plane local coordinate system and the double quotes the projected location on the reference plane.

On the wake reference surface the boundary conditions are also linearized, leading to the model in which the vortex lines form a system of parallel lines aligned with the x-axis of the geometry reference axis.

5.3 - Solution strategy.

In general an analytical solution of the boundary value problem does not exist, so the potential flow problem is solved numerically. The solution of the Prandtl-Glauert equation is expressed, using Green's theorem, into a surface boundary integral of elementary solutions (doublet and source singularity elements).

The geometry wetted surface is discretized into (quadrilateral) panels. The panels on the lifting surfaces are positioned on the reference plane. At fuselage-lifting-surface junctions, (non-wetted) segments are added to account for lift-carry over. At each (wetted) panel a collocation point (in subsonic flow the midpoint) is selected, where the normal flow boundary condition is imposed.

Next, each panel is assigned an elementary (source and/or doublet) solution, distributed over the panel surface with an as yet unknown strength. At each collocation point, the velocity components normal to the local surface, excited by each panel singularity, are summed and expressed in the unknown singularity parameters. This yields a set of equations, the left hand side being the Aerodynamic Influence Coefficients (A.I.C.) matrix multiplied with the column vector with the unknown singularity parameters and the right hand side (R.H.S.) equal to the component of the free stream velocity, normal to the local surface, a term due to the lifting surface camber, and a term due to the known source distribution accounting for lifting-surface thickness. The singularity parameters can now be solved for, followed by the computations of the velocity and pressure distributions.

6 - Geometry handling.

For the aerodynamic design problem, the most serious problem is how to express the pressure distribution as a function of the geometry alterations. Direct utilization of the panel method (without the lifting-surface approximation), by sequentially changing the geometry, and solving the pressure distribution for the new geometry leads to excessively high computational costs: for each variation of the geometry a new set of equations should be set up and solved. Typically, approximately 80% of the CPU time is spent on setting up the A.I.C. matrix, 5% on the R.H.S., 10% on solving the system of equations and 5% on the pressures and velocities. In the present method, two different techniques are employed to reduce the CPU time. Both methods leave the A.I.C. matrix intact and express the basic shape functions (variations in the geometry) in changes in the R.H.S. only.

6.1 - Non-lifting parts.

For non-lifting (engines, fuselage) components, the local geometrical changes are modeled using a transpiration velocity technique: Each affected panel remains on the baseline geometry, and

is assigned a yet unknown transpiration velocity which displaces the stream surface away from the baseline geometry. Due to this displacement, a (virtual) volume is created between the actual panel and its associated displaced stream surface, see fig. 1. The panel transpiration velocity

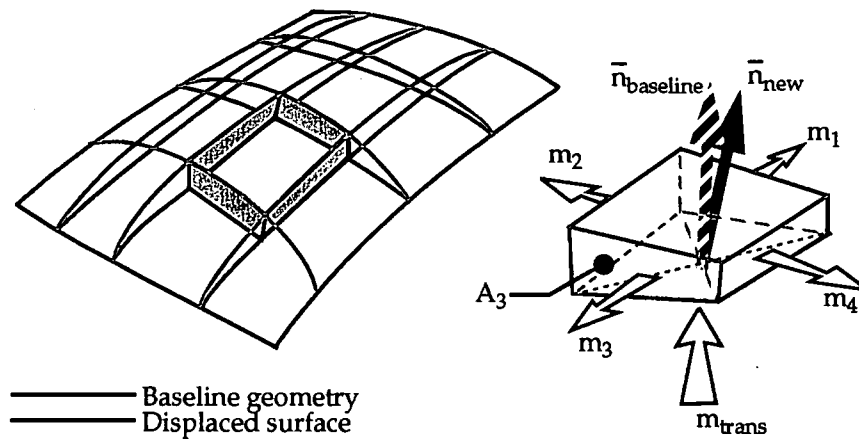


fig. 1: Wetted surface displacement, mass flux balance and normal vector disposition.

(m_{trans}) is found by balancing the flux ($m_1 \dots m_4$) through the boundaries of this volume, using the normal vector of the baseline geometry ($\bar{n}_{baseline}$):

$$(\bar{U}_\infty + \bar{u}_{trans}) \cdot \bar{n}_{j, baseline} A_{panel} = \sum_{i=1}^4 m_i = \sum_{i=1}^4 (\bar{U}_\infty + \bar{u}_i) \cdot \bar{n}_i A_i \quad (12)$$

Here, the mass flow is defined outward positive, except for m_{trans} . Note that only the outer stream surface has a zero mass flux, and the volume surfaces are not necessarily aligned with, or normal to the local stream lines and geometry. Furthermore, the new, outer stream surface has a normal vector that is not necessarily aligned with the baseline one. The local velocities ($\bar{U}_\infty + \bar{u}_i$) are interpolated from the data at adjacent panel midpoints and are depending on the transpiration velocity \bar{u}_{trans} . So \bar{u}_i is calculated iteratively. To account (partially) for the nonlinear effects, the pressure (variation) is then calculated imposing the boundary condition at the collocation point on the baseline geometry with the transpiration velocity (mass flux) magnitude based on the velocity distribution of the previous iteration cycle, combined with the tilted normal vector (\bar{n}_{new}) of the modified geometry.

6.2 - Lifting surfaces.

In the lifting surface approximation the boundary condition is expressed in terms of the camber and thickness slopes (eqn.(10)). A change in camber or thickness does not change the position of the collocations points. This simplification allows a very effective analysis of the pressure variations due to small geometrical changes. In effect, only the normal velocity condition, i.e. the R.H.S., needs to be updated, leaving the A.I.C. matrix unaffected. This kind of variation in geometry is implemented straightforwardly.

6.3 - Basic shape functions.

The basic shape functions are a means to construct displaced wetted surfaces, offering rather arbitrary geometrical variations, using a limited parameter set. Two basic shape functions are re-

quired to define a displaced surface, running in two independent directions. The natural choice is to span one basic shape function parallel to the (local) contours. For lifting surfaces the approximate directions are the chord and span directions, for body-like components the longitudinal (X-axis) and the circumferential ones.

The various types of basic shape functions are stored in a library (shape library) that is easily extensible. Among the type of basic shape functions stored in this library are: *sin* functions, providing Fourier series-like geometry changes, \sin^2 functions, "linear ramps" to simulate flap deflections (camber changes), Chebychev polynomials, especially useful if leading or trailing edges are to be modified, and finite element like linear functions. Several example basic shape functions are displayed in fig. 2, and example displaced surfaces in fig. 3. Note that the basic shape functions

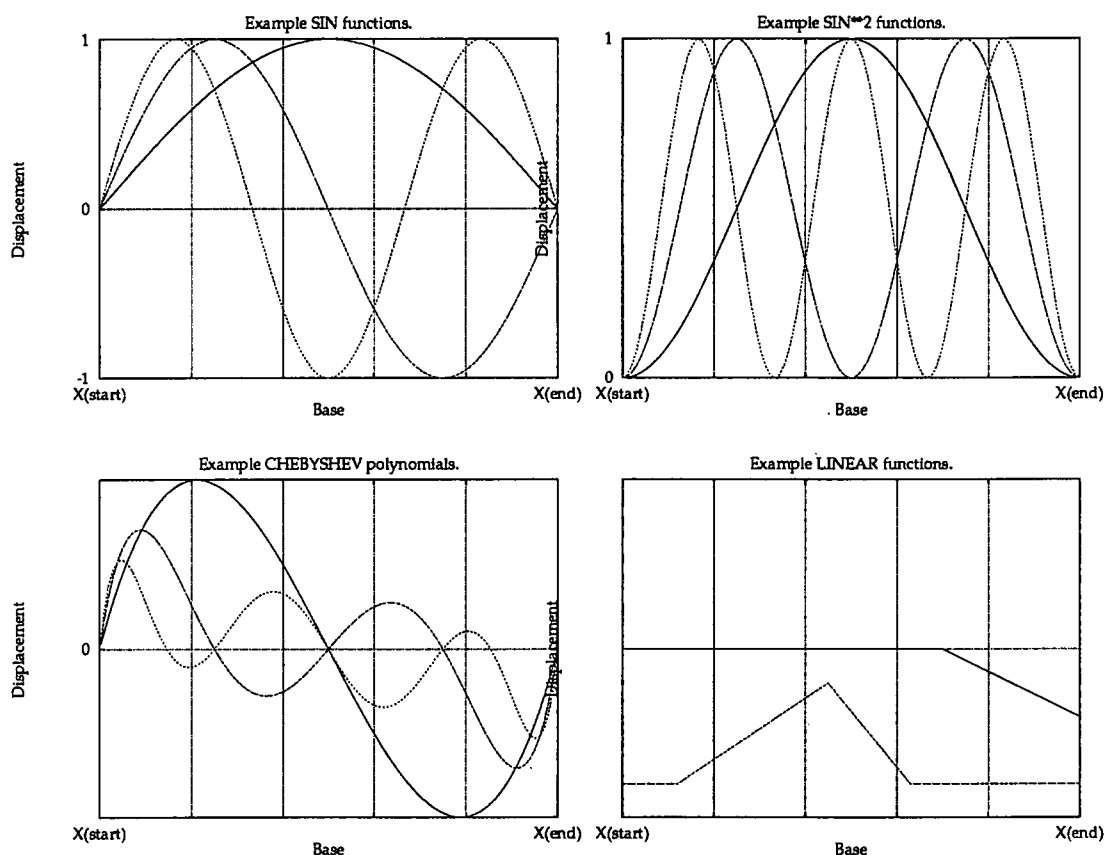


fig. 2: Basic shape function examples (dimensionless).

must satisfy certain requirements to ensure a fully closed wetted surface and to prevent (self-) intersections. However, this does not always mean that all basic shapes should have a zero displacement at their boundaries, notably camber modifications.

The displacement surfaces may be located anywhere over the geometry wetted surface: the edges of these surfaces do not have to coincide with leading and/or trailing edges. Moreover, the displacement surfaces are not restricted to a displacement normal to a wetted surface. For lifting surfaces the designer may opt for any combination of changes in thickness, camber, pressure or suction surface. At body-like surfaces the change in shape is usually normal to the local surface, but the designer may add constraints to force the changes in a prescribed direction.

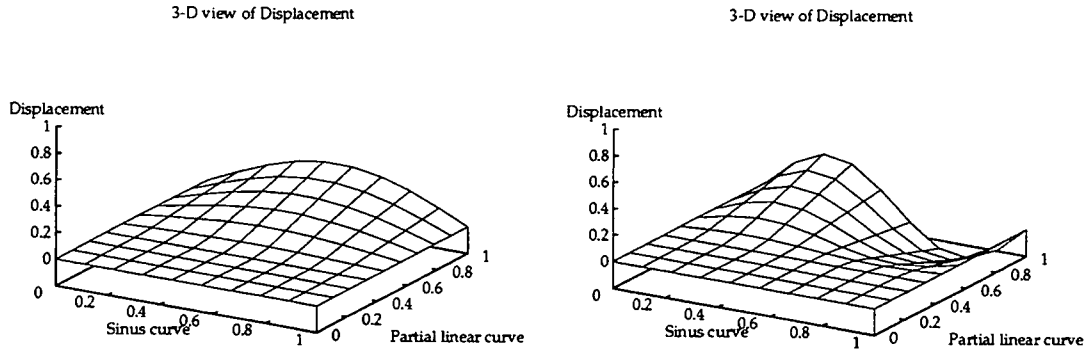


fig. 3: Example displacement surfaces (dimensionless).

7 - Finding a better geometry.

Once the user has determined what basic shape functions to use at which locations, has set target pressures at selected regions, and has assigned weight factors to each flight condition, a system of equations is set up, based on eqn.(1) through eqn.(4). The design problem is thus cast into a constrained least squares mathematical formulation:

$$\begin{bmatrix} e_{\text{ipanel, icase, ishape}} & \dots & \dots \\ \dots & \dots & \dots \\ \dots & \dots & \dots \end{bmatrix} \cdot \begin{bmatrix} \dots \\ A_{\text{ishape}} \\ \dots \end{bmatrix} = \begin{bmatrix} \text{rhs}_{\text{panel, icase}} \\ \dots \\ \dots \end{bmatrix}$$

$$e_{\text{ipanel, icase, ishape}} \equiv \sqrt{W_{\text{icase}} W_{\text{ipanel}}} \frac{\partial c_p}{\partial A_{\text{ishape}}} \Big|_{\text{ipanel, icase}} \quad (13)$$

$$g_{\min} \leq g_{\text{baseline}} + \sum A_{\text{ishape}} \Delta g_{\text{ishape}} \leq g_{\max}$$

$$\text{rhs}_{\text{ipanel, icase}} \equiv \sqrt{W_{\text{icase}} W_{\text{ipanel}}} \left(c_p \Big|_{\text{ipanel, icase}}^{\text{target}} - c_p \Big|_{\text{ipanel, icase}}^{\text{baseline}} \right)$$

For a unit change of each displaced surface, the changes in pressure coefficient at the target locations are determined and their effect onto the geometrical constraints determined. This leads to a system of equations with the amplitudes to be determined. Generally, the number of target pressures is unequal to the number of unknown basic shapes (amplification factors). The unknown amplitudes are solved for the minimum sum of the squares of the residuals (eqn.(2)).

If multiple solutions exist, i.e. more than one set of amplitudes exist that returns the minimum residual, that least squares solution is returned that yields the minimum geometrical change, i.e. the minimum length of the vector of shape amplitudes A_{ishape} . For this, a standard routine from the NAG⁽⁴⁾ library is used.

This formulation does account for the non-linear relation between the pressure coefficient, its derivatives and the geometry. After a solution for the amplitudes is obtained and the new geometry is conceived, the minimization process should be restarted, based on the updated geometry, until convergence is reached. Because the calculations of the pressures and its derivatives is quite resource demanding, it is left to the designer whether and when the pressure distribution, and/or its derivatives are updated.

8 - ADAS implementation.

The program package is designed to be implemented and operated on top of the Aircraft Design and Analysis System (ADAS⁽²⁾) environment. ADAS is a software tool developed at the Faculty of Aerospace Engineering of the Delft University of Technology for conceptual/preliminary design.

First a baseline design is put into ADAS format, essentially a three view, 2-D drawing. Starting from such a baseline definition, a 3-D grid over the wetted surface of the aircraft, called panel model, is generated using a dedicated grid generator. Several aerodynamic tools, e.g. panel methods, boundary layer methods, circulation optimization methods and geometry optimization methods, operate on this grid, as shown in fig. 4. Some of these tools are capable to analyze only

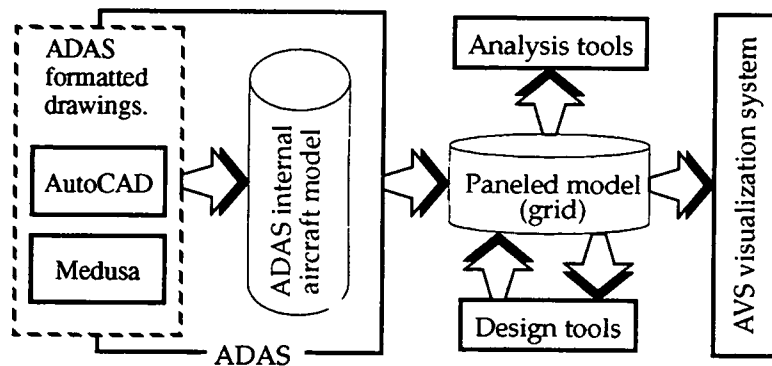


fig. 4: Organization of ADAS-Aerodynamic tools.

the paneled aircraft design (analysis of pressure distributions, lift, drag & moments), while other (design) tools are able to modify the geometry by changing the grid. This allows geometry refinement beyond the geometry definition capabilities of ADAS.

9 - The design procedure.

The design method is incorporated into a program package, and structured according to the design procedures usually adopted for this kind of design problems. This chapter will deal with both the design procedures and the programs within this package.

9.1 - A general approach.

The quest for the "optimal" aircraft aerodynamic shape geometry is distinguished by several steps, (fig. 5). Each of these steps will be explained in detail. At all stages, a graphics system informs the designer about (intermediate) results, and allows selection and manipulation of data.

- First, an aircraft design is conceived, formatted according to the ADAS standard, and accepted as the baseline geometry (fig. 6):
- From the baseline design a representative paneled model is generated, using the grid generator (panel program). This program, essentially a meshing like procedure, covers the wetted (and auxiliary) surfaces with panels and is capable of re-panelling a derivative of the baseline geometry in case the ADAS optimization or parametric variation option is invoked.
- The design flight conditions, e.g. cruise and climb, are set, i.e. the parameters such as Mach number, altitude, angle of attack, flight condition weight factor etc. specified. The weight factor is used to stress the relative importance of the flight conditions involved, and may be based

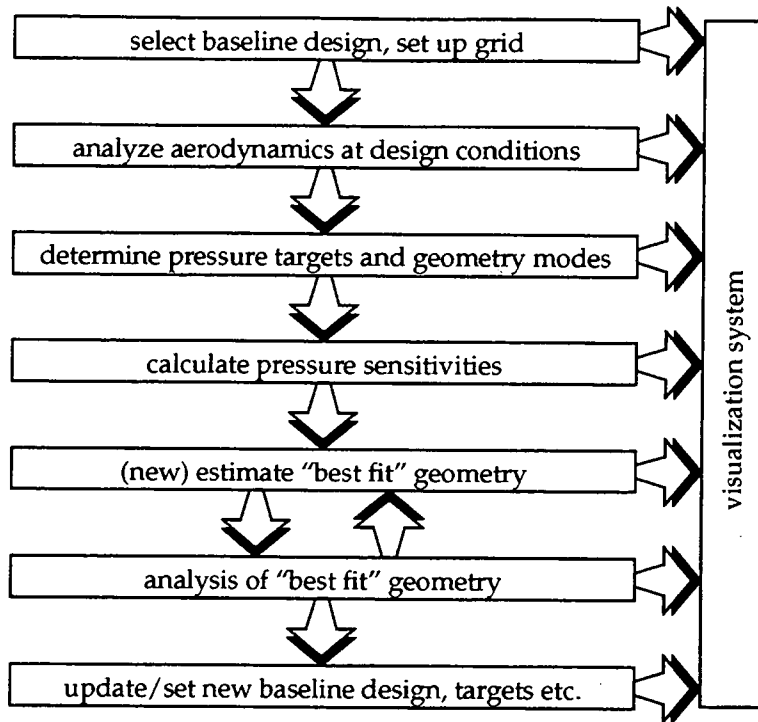


fig. 5: Basic design procedure steps.

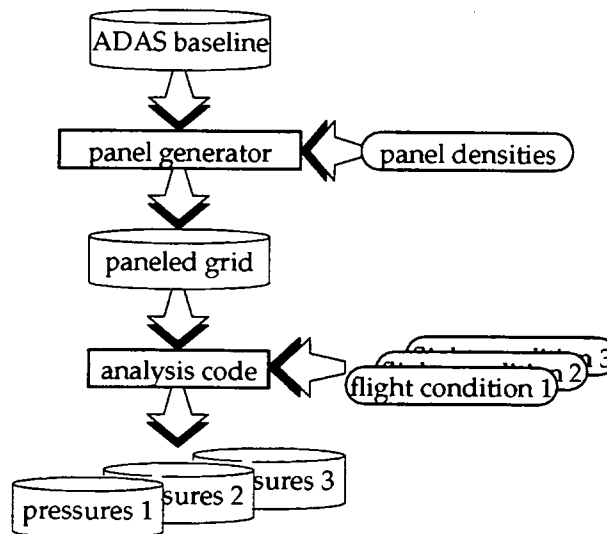


fig. 6: Baseline set up and analyses.

on e.g. the time spent in this flight condition. For each design flight condition, an aerodynamic analysis of the baseline design yields a baseline pressure distribution.

- Next, some design (experience based) decisions have to be made: the user should prescribe which parts of the wetted geometry are subjected to local geometrical refinement and, for each part, what kind of changes of the geometry are allowed by selecting a number of basic shapes

from the shape library (fig. 7). These decisions are not only affected by effectiveness (can the target be met), but are also depending on the (geometrical) design space. Optionally, upper and lower constraints in geometry changes are specified.

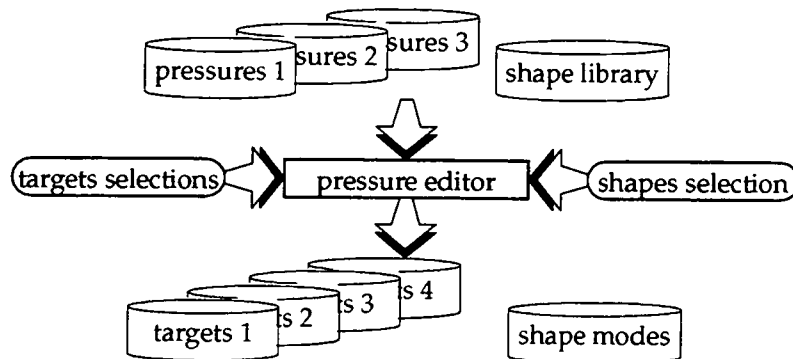


fig. 7: Determination of target pressures and geometry modes.

- Now, the designers intuition and experience is fed into the optimization process. For all flight conditions, the designer sets target pressures over parts of the wetted surface, and assigns a weight factor to each target pressure, to (de-) emphasize its relative importance. These target pressures hold the key for low drag, maximum lift, etc. The parts subjected to geometric changes and the parts over which a target pressures are prescribed are not necessarily the same. The location of target areas may even vary between the flight conditions.
- Next, the sensitivities of the pressure distributions at each target location are determined as a function of a unit change of each basic shape variation applied, for all the flight conditions defined (fig. 8).

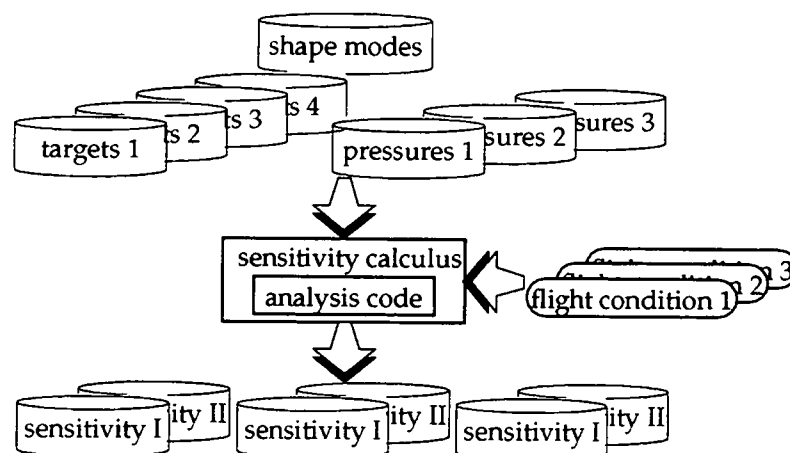


fig. 8: Calculus of sensitivities.

- Prior to entering the optimization stage, each flight condition itself is given a, mission dependent, weight factor.

- Next, the iterative optimization program is started. At each iteration, the amplitude of each basic shape is determined from a least squares optimization (fig. 9), based on the baseline (previous iteration) pressures for all flight conditions, its pressure sensitivities and the target pressures and weight conditions, as described in section 4. After finding the amplitudes, that

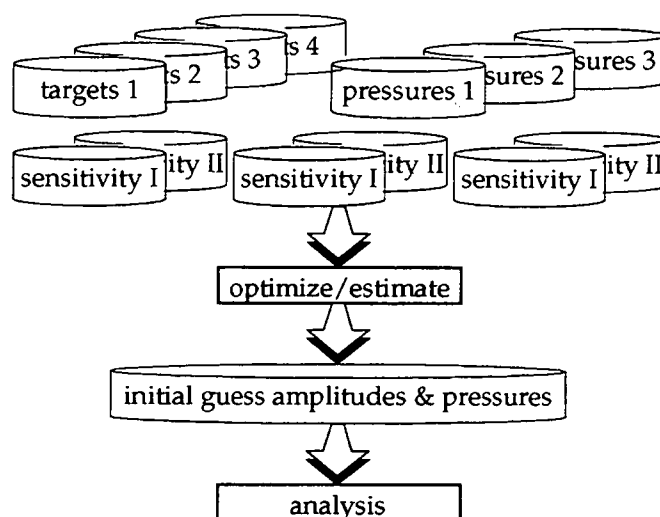


fig. 9: First step in optimization process.

may be constrained and multiplied by relaxation factors, as specified by the user to account for the nonlinear relation between pressure and shape variations, a new geometry is conceived. This geometry is initially mimicked by the baseline geometry with a displaced wetted surface using the transpiration technique for the body-like parts and the new camber and thickness distribution over the lifting parts ("soft geometry update"). The transpiration velocity distributions are different for all flight conditions and are used to estimate the overall pressure distribution due to the combined nonlinear effects of all shape changes simultaneously. At the next iteration, the amplitudes, pressure and normal flow distributions are updated again and the geometry analyzed again until either the maximum number of iterations or the convergence criterion is met (fig. 10). This new, transpiring geometry consists of the baseline design and a displaced surface, with flight conditions depending transpiration velocity distributions. Depending on the designers judgement, this "soft optimization" step may be repeated or the next step invoked.

- After finding a proper relaxation factor and/or amplification factors, the resulting new, transpiration geometry is then transformed into a new baseline geometry, with zero transpiration displacements: For the non-lifting surfaces, the geometry is displaced, by actually moving the wetted surface to the displaced one ("hard update"). This requires a recalculation of the A.I.C.'s. For lifting surfaces a new camber and thickness distribution is set. Effectively, this step and the preceding one are a two step method to update the non-lifting surfaces: the preceding step changes the normal flow condition, while preserving the locations where these conditions are imposed. The current step moves these locations to the new, wetted surface.
- This new baseline is the start of a new iteration cycle. At this stage, usually the virtual, displaced transpiration surfaces are replaced by the new body surface geometry which it is simulating. This requires calculation of the A.I.C. matrices again. At this point, the user determines whether the new, refined geometry exhibits satisfactory pressure distributions. This refined geometry may be accepted or a new design cycle may be invoked, which may start anywhere. The process may continue with:
 - another iteration, starting with a new least squares optimization step, or,

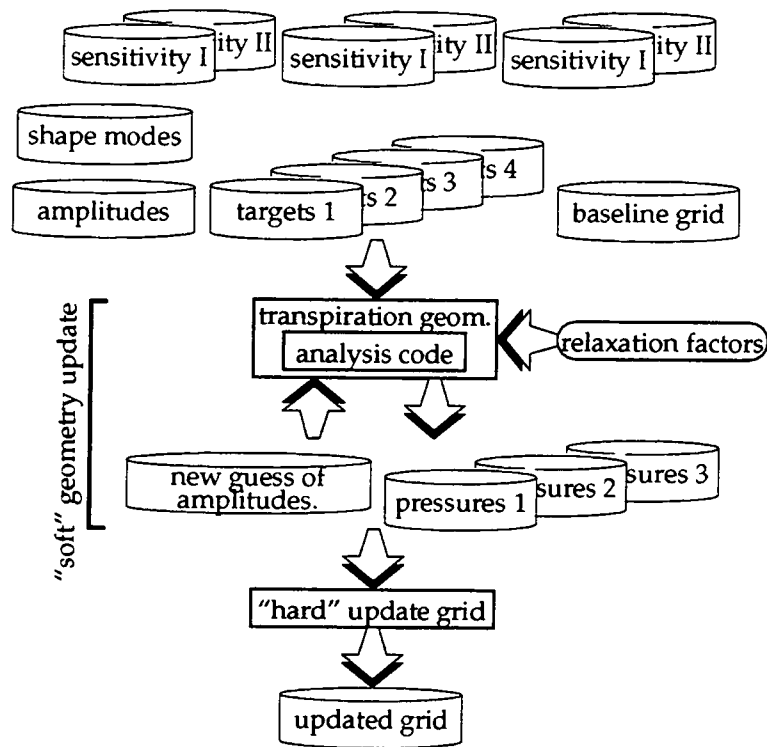


fig. 10: Second update in single iteration.

- compute the sensitivities again, or,
- change/add/remove basic shape functions, or,
- change/add/delete target pressures and geometry constraints, or,
- as a last resort: re-panel the current baseline design, or even select a different baseline.

10 - A showcase.

To show the versatility and power of this inverse design tool, a wing-fuselage combination will be analyzed and refined, using the procedure as laid out in fig. 5. The wing pressure side surface and the fuselage surface just below the fuselage-wing junction will be refined, driven by a prescribed chordwise pressure distribution over the wing lower surface, next to the junction.

10.1 - Baseline design and flight conditions.

The baseline design is defined using the ADAS/Medusa format, as in fig. 11. This drawing shows the minimum geometrical definition required to define the aircraft wetted surfaces. For this purpose, the engines and all internal entities, including cabin and structural layout are not (yet) defined.

Two typical design flight conditions are chosen: a cruise and a climb condition, the relevant parameters are:

Now a computational grid over the wetted (and auxiliary) surfaces must be generated (fig. 6): the ADAS drawing is read by a dedicated grid generator that panels the geometry semi-automatically. This program asks the user for the number of spanwise contours and chordwise number of

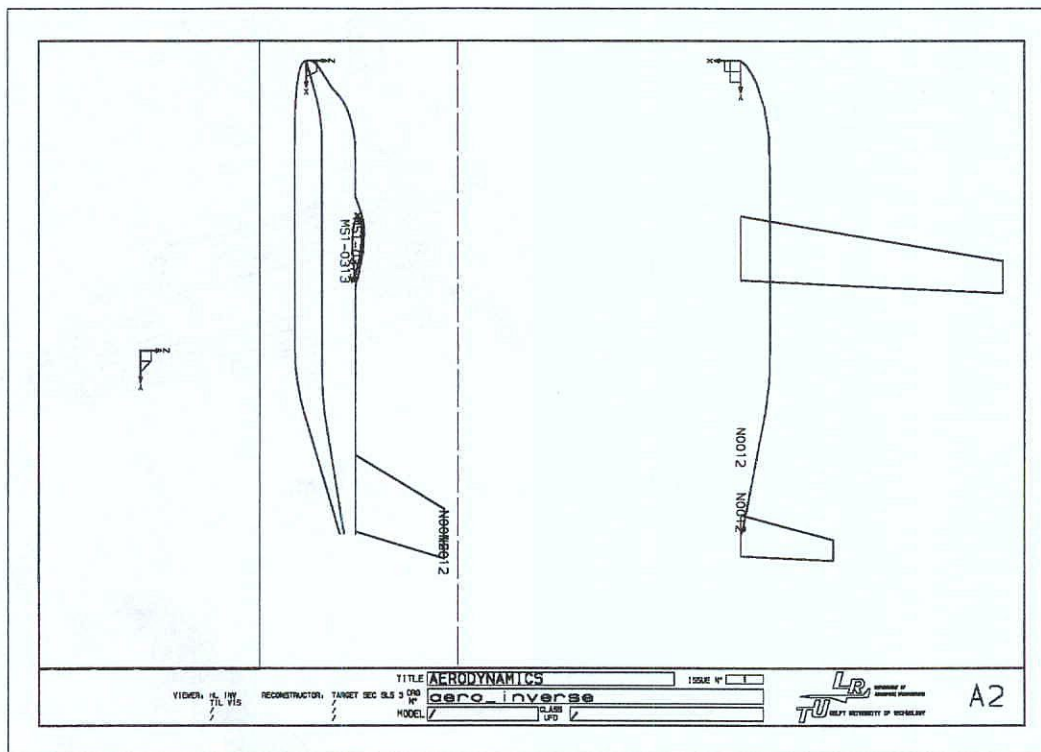


fig. 11: ADAS (minimum) geometry definition.

(Input) Parameters	Cruise	Climb	Unit
Altitude (S.A.):	7000.0	0.0	m
Free stream mach number:	0.35	0.2	-
Angle of attack:	0.0	5.0	deg.
Weight factor flight condition:	2.0	1.0	
Resulting configuration lift coefficient (C_L):	0.43	0.87	-

Table 1: Design conditions.

points for the wing, and for the fuselage the number of circumferential points and the number of contours of the nose and tail sections. The contour and point distributions over the fuselage sections above and below the wing are automatically determined. The resulting panel distribution is depicted in fig. 12. Note that the forward and aft fuselage are covered with rather large panels. At those places a crude panelling will suffice for the present purpose. This picture shows the lifting surfaces as camber surfaces, the thickness distribution is not shown. A small fuselage fairing covers the wing camber surface. The overall pressure distributions for the climb condition is shown in fig. 13.

10.2 - Selection of geometry variations and pressure targets.

Next, the designer has to decide over which parts of the geometry the pressure distributions are unacceptable and need improvement (fig. 7). At those locations, (improved) target pressure dis-

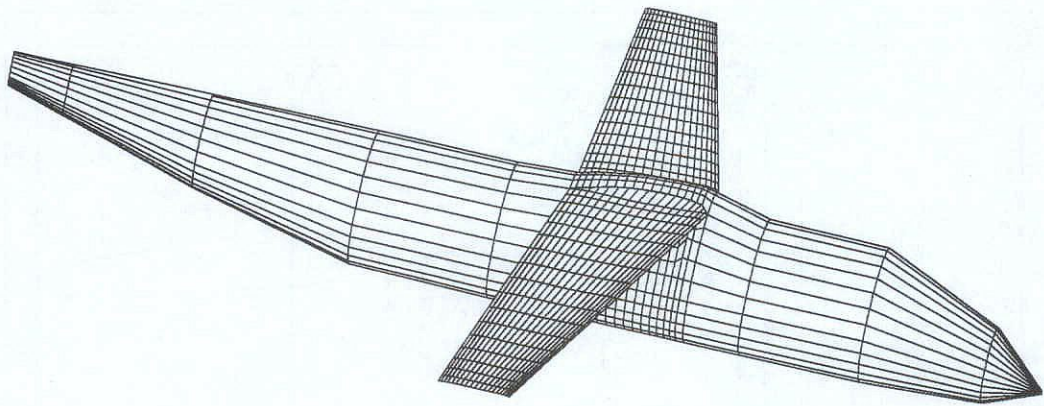


fig. 12: Paneled aircraft baseline configuration.

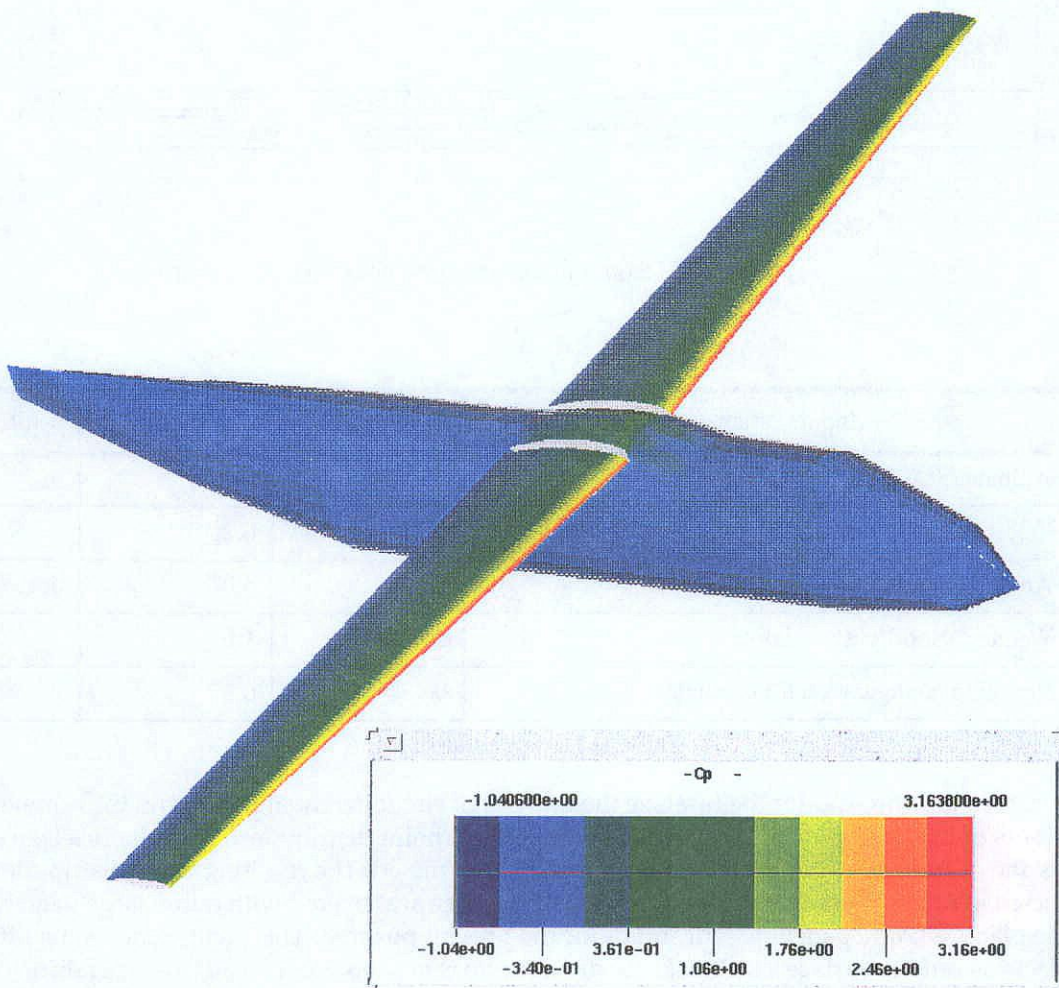


fig. 13: Pressure distribution over the baseline at climb condition.

tributions have to be specified. In this study, the target pressures at the inboard wing lower surface just outboard of the fuselage are set equal to the pressures at the same positions of the same wing without the fuselage interference effects. The discussion on whether this choice is justified

is not within the scope of this report. The baseline and target pressures are depicted in fig. 14 (cruise condition) and fig. 15 (climb condition). Note that for each flight condition, multiple target

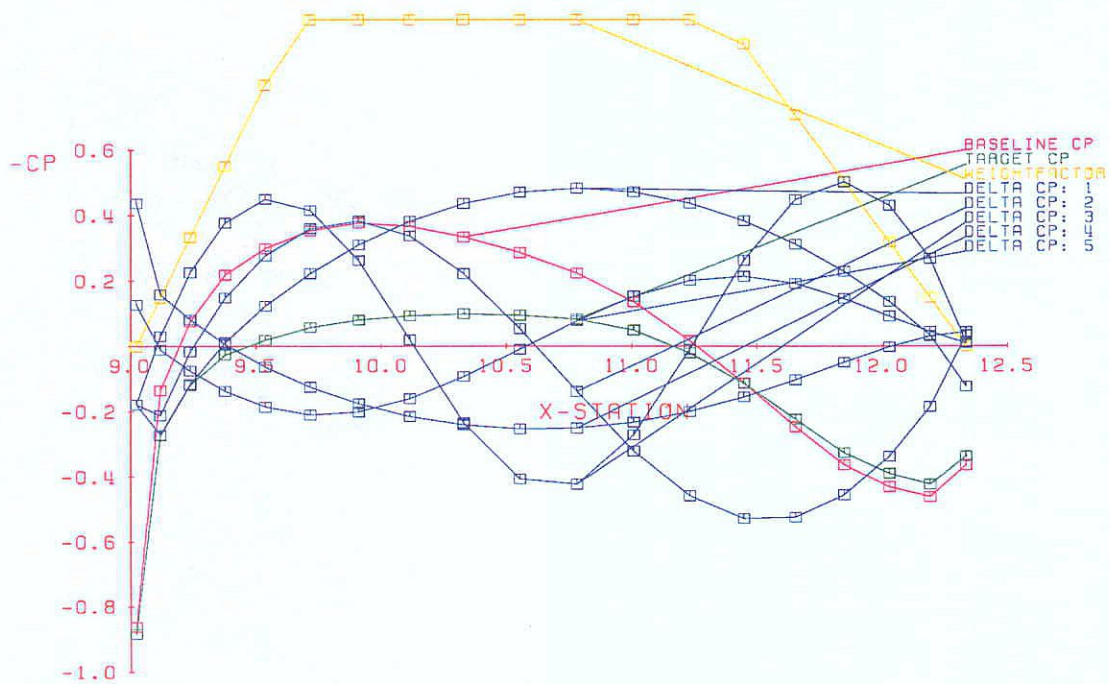


fig. 14: Baseline, incremental and target pressures at cruise condition.

pressures are defined, independent from the other flight condition.

Simultaneously weight factors are defined. Weight factors are a means for the designer to emphasize the importance whether a target pressure is met at each target location. However, there is an additional consideration. Near the wing leading edge the pressure coefficients are calculated with relative high inaccuracy due to violation of the assumptions underlying the lifting surface approximation. Hence, a natural choice is to specify lower values of the weight factor near the wing leading edges.

Next, the user selects the parts of the geometry that are subjected to geometrical changes. In this study, the lower surface of the inboard wing and the fuselage just below the fuselage-wing junction are selected: At the wing lower surface, three (for industrial applications too few) displacement modes are chosen. In chordwise direction three basic shapes (*sin* functions) are selected. These displacements are fading out linearly towards the tip. The displacement surfaces of the fuselage lower junction are spanned by two sinus basic shapes in approximately free stream direction and a linear ramp in circumferential direction, starting at the maximum width with its maximum at the wing-fuselage intersection. Note that for all flight conditions the geometrical changes are the same. Example displacement modes, a fairing on the fuselage at the wing root, and a sinus shape over the lower surface of the inboard wing, are shown as displaced surfaces in fig. 16. For visualization purposes, the displacements are magnified, the colors are a measure for the magnitude of displacement.

Once the designer has completed the previous steps, the variations of the pressures due to the basic shape unit changes can be determined (fig. 8). Fig. 14 and fig. 15 show the pressure variations due to a unit variation of the basic shapes to the baseline design.

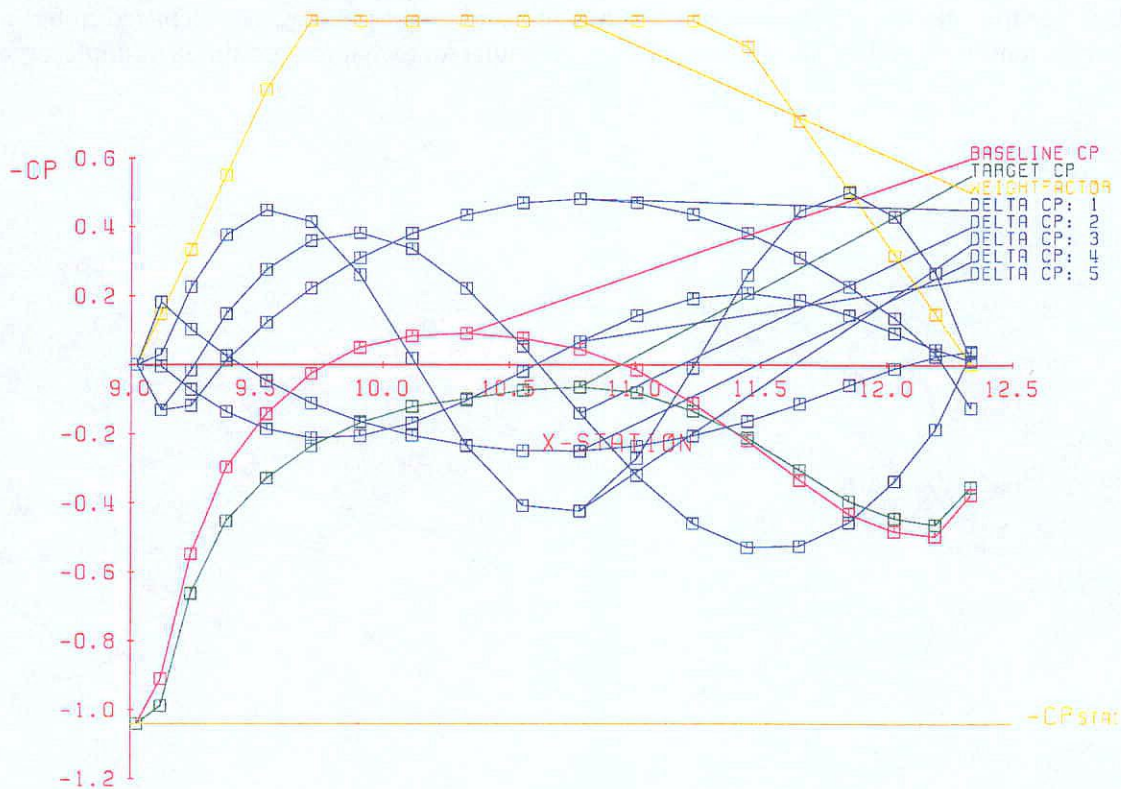


fig. 15: Baseline, incremental and target pressures at climb condition.

10.3 - The optimization step.

Next the optimization step is invoked (fig. 9 and fig. 10). The optimizer estimates the amplitudes of each basic shape, using the least squares minimization procedure. The optimizer gathers all sensitivity data automatically. After each estimate, the pressure distribution of the resulting, new geometry is calculated again, using the baseline geometry with the newly determined displaced wetted surfaces. Based on the updated pressure and velocity distributions, a new estimate of the displacement amplitudes can be made. This process can be repeated until convergence or the designer decides to use a new set of pressure sensitivities. Once the optimization loop is exited, a new, updated baseline geometry can be created from the old baseline one and the displaced surfaces.

10.4 - Final results.

After a single full design iteration, i.e. one baseline, one set of geometry modes, two sets of flight conditions, with calculation of only one set of pressure sensitivities and 6 iterative optimization cycles, the target and actual pressure distributions are fairly close, see fig. 17 and fig. 18. The cross sections at the wing root and the fuselage just below the wing-fuselage junction are shown in fig. 19 and fig. 20. Fig. 19 shows the projections of a strip of fuselage panels, just below the wing-fuselage junction onto the X-Z and X-Y reference planes. A 3-D view of the baseline and resulting, updated geometry are shown in fig. 21. At this stage the new baseline is ready for further refinement.

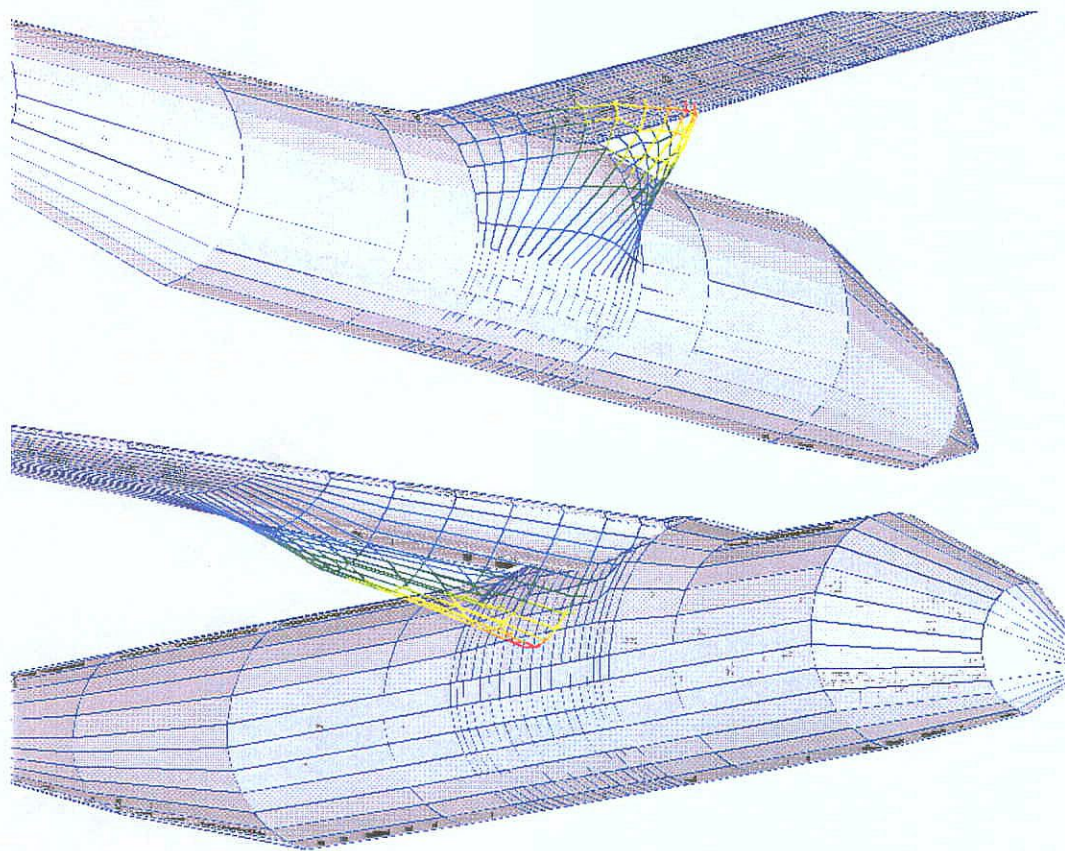


fig. 16: Two example unit displacement modes (20 x enlarged, colors denote displacement), superimposed over the baseline geometry (in grey).

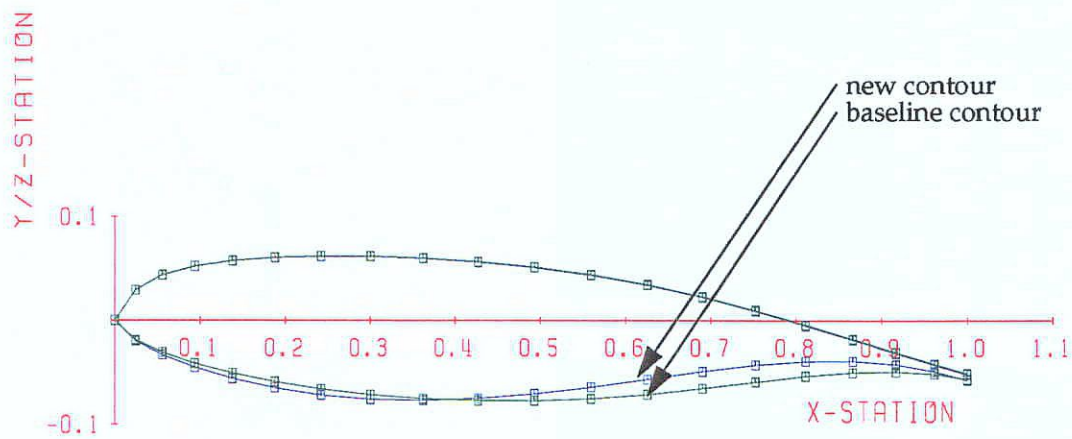


fig. 20: Baseline and refined cross section.

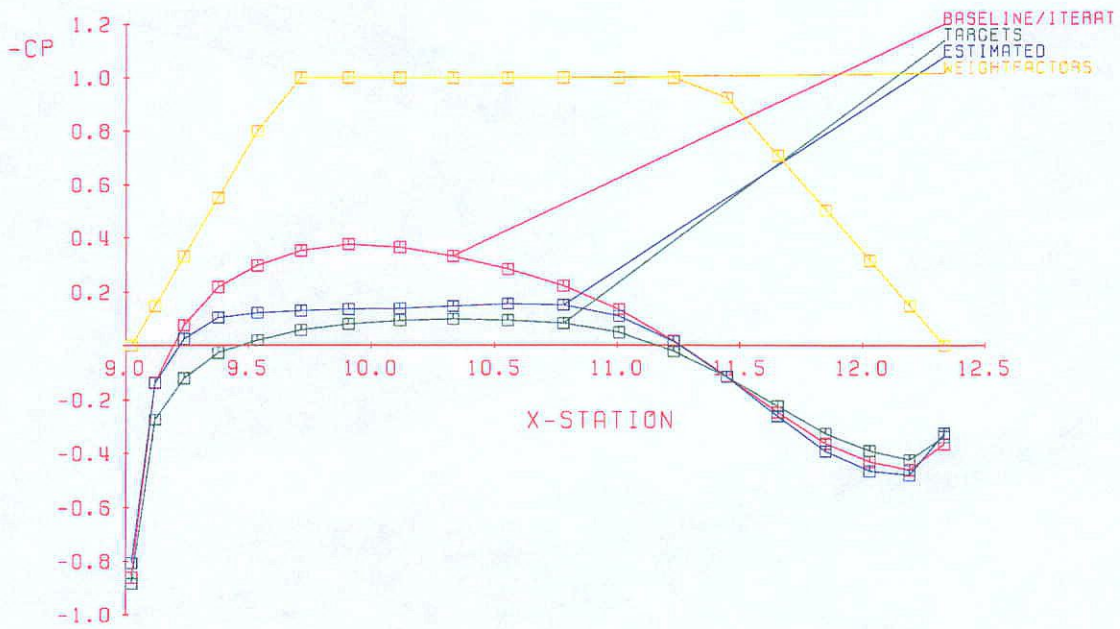


fig. 17: Final, emulated and target pressures for cruise condition.

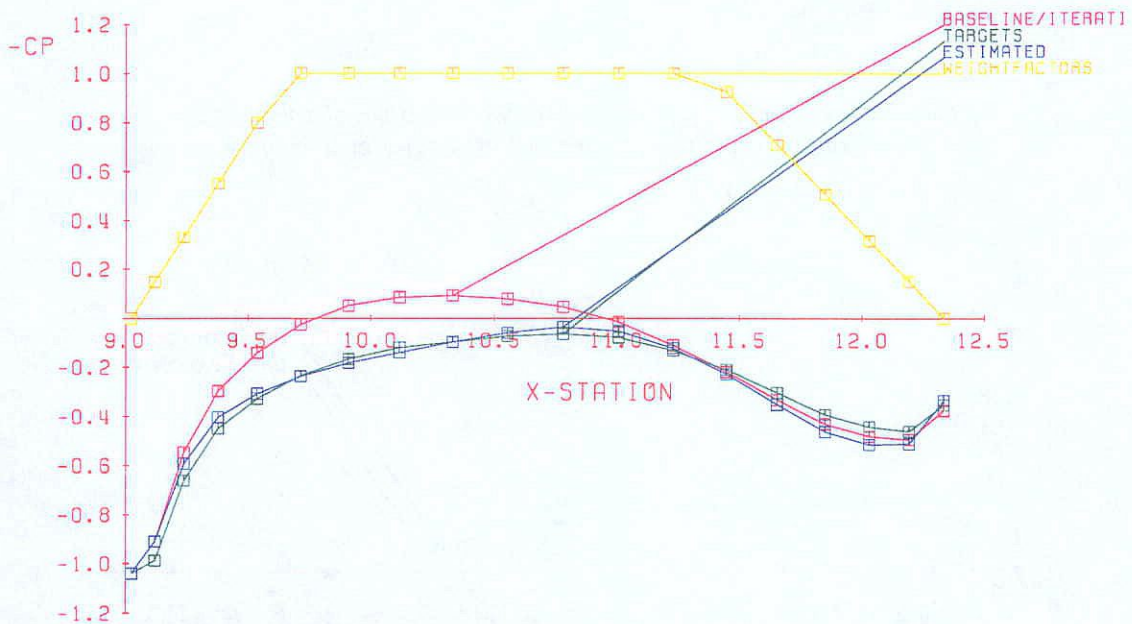


fig. 18: Final, emulated and target pressures for climb condition.

11 - Concluding remarks.

This design tool is developed to determine the best fit geometry for prescribed pressure distributions at various target locations for complex 3-D configurations. It allows to refine an aircraft ge-

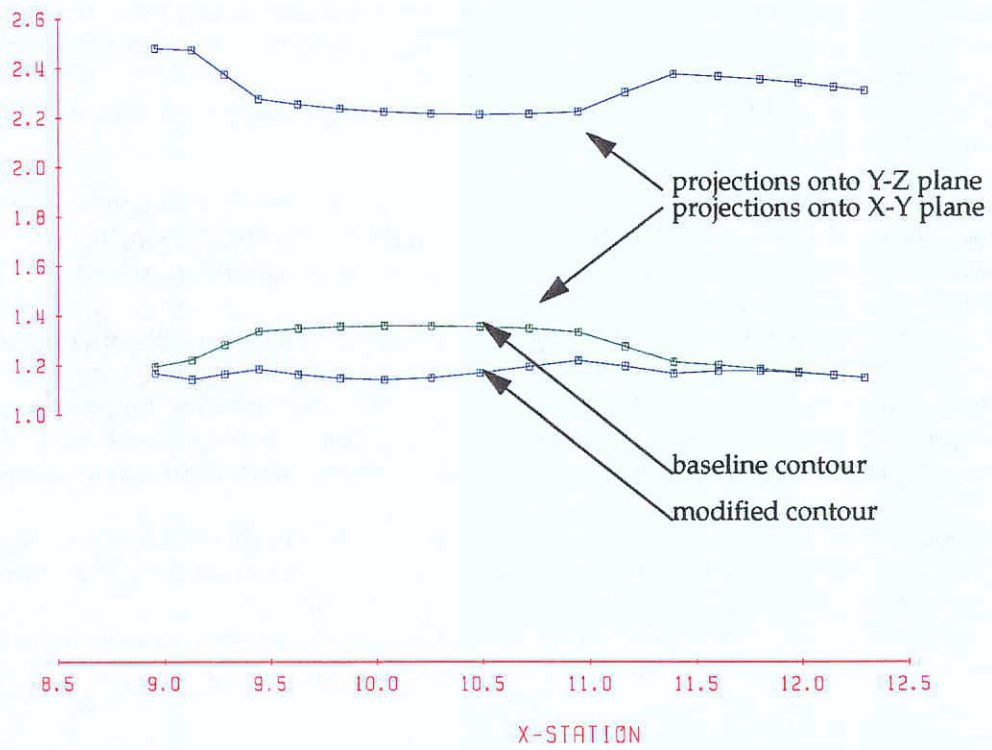


fig. 19: Baseline and refined fuselage geometry just below wing junction.

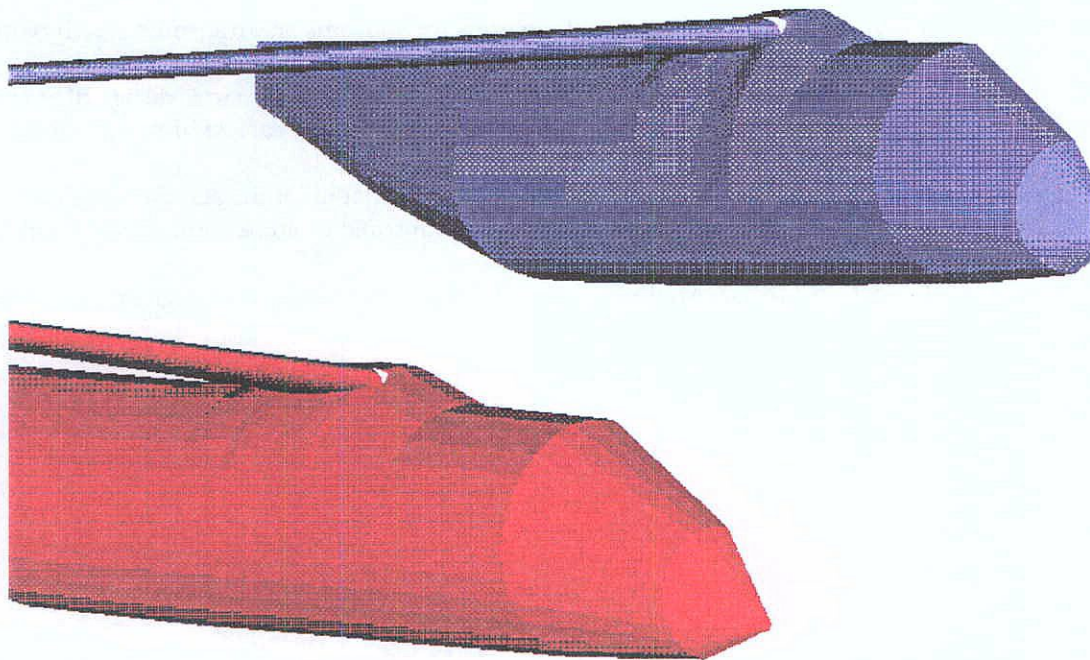


fig. 21: View of baseline and updated geometry.

ometry at several locations over several flight conditions simultaneously, while the designer has full control over the (changes in) geometry by selecting appropriate basic shape functions as well as imposing direct constraints on the geometrical changes.

However, the aerodynamic designer sometimes might get unexpected, unrealistic results or unwanted side-effects:

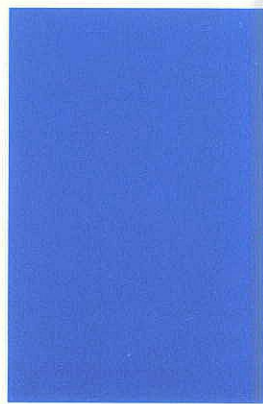
- A single change in the geometry principally affects the pressure distribution everywhere: The designer should check whether the resulting overall pressure distribution, lift and drag is acceptable. Unfavorable pressure changes may be counteracted through specification of additional target pressures.
- The program does not contain any design information and experience. The user is responsible for feeding this into the system. The design information consists of the prescription of those combinations of basic shape functions, geometrical constraints and target pressures and weight factors that produce feasible results, and, improves the aircraft aerodynamics, i.e. low drag, high maximum lift etc. Selecting unfavorable combinations might lead to suboptimal results.
- Although the number of applied basic displacement surfaces can be very large, it is recommended to start with a small set. In general this speeds up the overall design performance and prevents high frequency oscillations in the geometry surfaces.
- After optimization, it may be necessary (and at least recommended) to smooth the resulting geometry to get rid of the small oscillations in the geometry surface.

12 - Acknowledgments.

The software contains parts of the NLRAERO panel method, notably the A.I.C. and the R.H.S. calculations. NLRAERO is developed by the Dutch National Aerospace Laboratory (NLR), Amsterdam.

13 - References.

- 1- Slooff, J.W.: "A survey of computational methods for subsonic and transonic aerodynamic design." NLR MP 84066 U.
- 2- Middel, J.: "Development of a computer assisted toolbox for aerodynamic design of aircraft at subcritical conditions with application to three-surface and canard aircraft." Doctoral thesis. Delft University Press, ISBN 90-6275-768-5 / CIP.
- 3- Hoeijmakers, H.W.M.: "A panel method for the determination of the aerodynamic characteristics of complex configurations in linearized subsonic or supersonic flow." NLR TR 80124 U
- 4- an.: "NAG Fortran Library Manual, mark 15 volume 6." Numerical Algorithms Group Limited. ISBN 1-85206-070-0.



Rapport 803



60141050812

965150